

**THE EFFECT OF SHOCK ON THE AMORPHOUS COMPONENT IN ALTERED BASALT** S. A. Eckley<sup>1</sup>, S. P. Wright<sup>2,3</sup>, E.B. Rampe<sup>4</sup>, and P.B. Niles<sup>4</sup>, <sup>1</sup>Jackson School of Geological Science, University of Texas, Austin, TX (seckley@utexas.edu), <sup>2</sup>Department of Geology and Environmental Science, University of Pittsburgh, Pittsburgh, PA, <sup>3</sup>Planetary Science Institute, Tucson, AZ, <sup>4</sup>Astromaterials Research and Exploration Science, NASA-Johnson Space Center, Houston, TX.

**Introduction:** Investigation of the geochemical and mineralogical composition of the Martian surface provides insight into the geologic history of the predominantly basaltic crust. The Chemistry and Mineralogy (CheMin) instrument onboard the Curiosity rover has returned the first X-Ray diffraction data from the Martian surface [1]. However, large proportions (27 ± 14 with some estimates as high as 50 wt. % [1,2]) of an amorphous component have been reported. As a remedy to this problem, mass balance equations using geochemistry, volatile chemistry, and mineralogy have been employed to constrain the geochemistry of the amorphous component [1,2]. However, “the nature and number of amorphous phases that constitute the amorphous component is not unequivocally known” [2]. Multiple hypotheses have been proposed to explain the origin of this amorphous component.

- Allophane (Al<sub>2</sub>O) [1,3]
- Basaltic glass (Volcanic and impact) [1,3,4,5]
- Palagonite (Altered basaltic glass) [1,3,4,5]
- Hisingerite (Fe<sup>3+</sup>- bearing phyllosilicate) [1]
- S/Cl-rich component (sulfates and/or akaganeite) [1,2,4,5]
- Nanophase ferric oxide component (npOx) [1,4,5]

Establishing a multi-phase amorphous component from a basaltic precursor that has undergone physical and chemical weathering within geochemical constraints is of paramount importance to better understand the composition of a large portion of the Martian surface (up to 50 wt. %).

Shocked basalts from Lonar Crater in India are valuable analogs for the Martian surface because it is a well-preserved impact crater in a basaltic target [6]. Having undergone pre- and post-shock aqueous alteration, these rocks provide crucial data regarding the effect of shock on the amorphous component in altered basalt. By conducting mass balance equations similar to what has been performed for Gale crater materials [1-5], we attempt to calculate the geochemistry of the amorphous component in altered basalts ranging from

Class	Petrographic Description
1 <20 GPa	Grains are fractured
2 20-40 GPa	Plag. transformed to maskelynite
3 40-60 GPa	Plag. transformed to a flowing glass of plag. composition
4 60-80 GPa	Plag. converted to vesicular glass; pyx melted on crystal edges and/or heavily fractured
5 >80 GPa	Plag. and pyx. completely melted

**Table 1:** Classes of shocked basalt with petrography (adapted from [6])

unshocked to Class 5 (Table 1) [6]. This has the potential to reveal the nature and origin (*i.e.* primary igneous, shock metamorphic, and/or aqueous alteration occurring before or after the impact event) of the amorphous component in shocked basalt with the goal of unravelling the history of the Martian surface.

**Methods:** Shocked and unshocked basaltic samples from the Lonar Crater, located within the Deccan Traps, were acquired by Dr. Shawn Wright during multiple field seasons. A complete range (unshocked/unaltered to Class 5 [6-8]) were found along the crater walls and in the ~1 m thick suevite matrix surrounding the crater. We acquired whole rock geochemical data on twenty-seven samples at the XRF laboratory at Franklin and Marshall. Powder XRD data were collected at NASA’s Johnson Space Center with crystalline phases and abundances determined using the HighScore Plus and Jade software; high-precision amorphous abundances were determined using the internal standard method (sample mixed with 20 wt. % corundum).

*Mass-balance equations.* To quantify the amorphous component, we utilized a technique modeled after [5], where we determine the difference in geochemistry between the bulk and crystalline to obtain the amorphous geochemistry. After retrieving specific

$$Oxide_{Bulk} - [Oxide_{Crystalline}] = Oxide_{Amorphous}$$

$$Oxide_{Bulk} - [\sum y_m * x_m \text{ with } \sum x_m = 1] = Oxide_{Amorphous}$$

chemical formulae for the crystalline phases, we calculated the elemental abundance (wt. % oxide) ( $y_m$ ) in each mineral. Next, we calculated a weighted sum of each oxide in a given rock by multiplying the abundance of a given oxide in each mineral ( $y_m$ ) by the abundance of each mineral ( $x_m$ ) in the bulk rock (amorphous included). These weighted oxide sums were subtracted from the bulk oxide geochemistry to return the geochemistry, in wt. % oxide, of the amorphous component in each rock. Necessary corrections were used for negative amorphous values and these corrected values were renormalized (Table 2).

**Results and Discussion:** The XRD analyses indicated a variety of phases within the twenty-seven samples: andesine, augite, pigeonite, quartz/cristobalite, hematite, magnetite, ilmenite, calcite, zeolites, vermiculite, and a range of hydrated phyllosilicates. In addition to crystalline phases, a broad amorphous hump was reported for most rocks above the Class 1 shock level. Samples LC04-056, LC09-235, LC09-327, and LC05-melt were selected for mass-balance calculations.

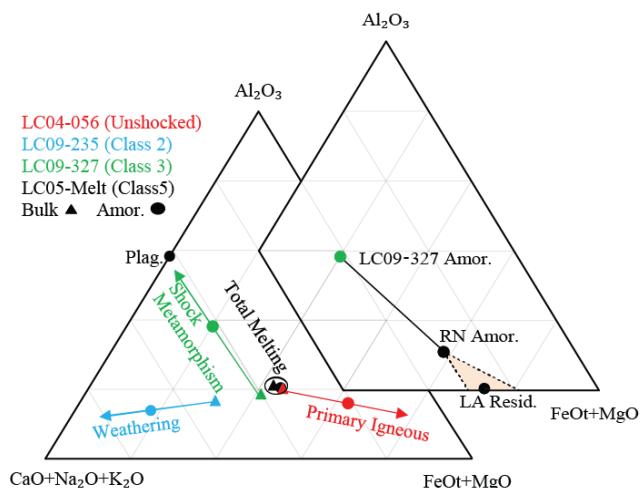
Oxide	LC04-056 (Unshocked)		LC09-235 (Class 2)	
	Crystalline	Amorph.	Crystalline	Amorph.
SiO <sub>2</sub>	62.89	9.22	47.43	46.28
TiO <sub>2</sub>	0.30	7.97	0.51	3.29
Al <sub>2</sub> O <sub>3</sub>	13.24	16.99	15.93	9.60
FeO <sub>T</sub>	5.26	37.17	9.46	14.51
MnO	0.07	0.72	0.00	0.32
MgO	4.46	14.25	11.49	0.00
CaO	10.93	11.82	11.16	24.56
Na <sub>2</sub> O	2.85	0.00	1.03	2.35
K <sub>2</sub> O	0.00	1.01	3.00	0.00
P <sub>2</sub> O <sub>5</sub>	0.00	0.85	0.00	0.35
TOTAL	100.00	100.00	100.00	100.00

Oxide	LC09-327 (Class 3)		LC05-Melt (Class 5)	
	Crystalline	Amorph.	Crystalline	Amorph.
SiO <sub>2</sub>	46.94	49.69	51.24	50.48
TiO <sub>2</sub>	2.34	2.39	0.00	3.79
Al <sub>2</sub> O <sub>3</sub>	1.18	21.07	17.08	12.01
FeO <sub>T</sub>	14.55	13.11	9.58	16.39
MnO	0.00	0.35	0.00	0.31
MgO	14.27	0.00	5.81	4.92
CaO	20.40	9.54	13.28	9.32
Na <sub>2</sub> O	0.31	3.17	3.01	1.34
K <sub>2</sub> O	0.00	0.35	0.00	1.06
P <sub>2</sub> O <sub>5</sub>	0.00	0.33	0.00	0.37
TOTAL	100.00	100.00	100.00	100.00

**Table 2:** Calculated oxide geochemistry (wt. %) for the crystalline and amorphous components, renormalized to 100 %

These samples had the best fit refinement patterns and contain 7.0, 29.0, 49.9, and 63.3 wt. % amorphous material, respectively. The data from Table 2 were converted to molar % and plotted on an A-CNK-FM ternary diagram (Figure 1) [9] to illustrate mixing and weathering of primary igneous phases [10]. Mixing lines connecting the bulk and amorphous geochemistry represent the evolution of the amorphous component from the bulk rock by various geologic processes. LC04-056 (unshocked) has 7 wt. % amorphous material, thought to be a primary feature formed during natural igneous processes. LC09-235 displays a weathering trend that could be the result of pre- or post-shock alteration. LC05-melt shows homogenization of both the amorphous and crystalline components, expected with an impact melt. Finally, LC09-327 has the most interesting process of amorphous component generation: shock metamorphism. This is a Class 3 shocked basalt where plagioclase is transformed beyond



**Figure 1:** Left: Bulk and amorphous geochemistry (molar %) for the four calculated samples with arrows representing the hypothesized processes by which the amorphous components were derived. Right: Rocknest amorphous component (RN Amor.) represented as a physical mixture between a shock-induced amorphous phase (LC09-327 Amor.) and a complementary amorphous phase(s) derived from weathering of basalt. LA Resid. (an acidic weathering residue [5 wt. % FeTi-oxides added in]) [10] is a possible candidate.

maskelynite into a flowing glass with an identical composition [6]. Therefore, a mixture of the bulk rock and plagioclase compositions comprise the resulting amorphous component. Plagioclase becomes relatively enriched in an impact breccia through preferential comminution from the target-rock during an impact [11]. Thus, relatively recent impacts (< 1 Ga) could produce significant amounts of plagioclase-composition amorphous material within the ejecta and become an integral part of the global Martian dust through aeolian homogenization [12,13]. Therefore, we hypothesize that the Rocknest amorphous component could be a mixture of this shock-induced plagioclase-glass/bulk rock combination (LC09-327 Amor.) and another amorphous weathering product.

**Conclusions:** Figure 1 demonstrates that by using our mass balance methods, different geologic processes can be identified. Furthermore, if this plagioclase/bulk rock amorphous phase (LC09-327 Amor.) is part of the Rocknest amorphous component, then the remaining amorphous material would be composed of Si, Fe, Mg, Ca, Na, K, and volatiles (S and Cl). One possible mechanism for the formation of material with this composition is by incipient weathering of basalt at low pH [10]. These chemical relationships provide an intriguing foundation for further research on how shock has affected the Martian surface.

**References:** [1] Bish D. L. et al. (2013) *Science*, 341.6153 [2] Morris R. V. et al. (2014) *LPSC 45 #1319* [3] Blake D. F. et al. (2013) *LPSC 44 #1289* [4] Morris R. V. et al. (2013) *LPSC 44 #1653* [5] Dehouck E. et al. (2014) *JGR 119*, 2640-2657 [6] Kieffer S. W. et al. (1976) *LPSC 7*, 1391-1412 [7] Wright et al. (2011), *JGR-Planets* [8] Goliber et al. (2017) *LPSC 48* [9] Nesbitt H. W. and Young G. M. (1982) *Nature*, 715-717 [10] Hurowitz J. A. et al. (2006) *JGR 111*, E2 [11] Reagan et al. (1996), *GSA 302*, 235-243 [12] McSween H. Y and Keil K. (2000) *GCA*, 64, 2155-2166 [13] Burns R. G. (1993) *GCA*, 57, 4555-4574.